

The $\text{Cu}_2(\text{C}_6\text{H}_5\text{NNNC}_6\text{H}_5)_2$ Dimer. Theoretical and Spectroscopic Investigations of the First Example of a Fluorescent $d^{10}-d^{10}$ Complex

Pierre D. Harvey

Département de chimie, Université de Sherbrooke, Sherbrooke, Québec J1K 2R1, Canada

Received June 23, 1994[Ⓞ]

The nature of the lowest energy singlet excited state of the $d^{10}-d^{10}$ $\text{Cu}_2(\text{C}_6\text{H}_5\text{NNNC}_6\text{H}_5)_2$ complex has been described theoretically by extended Hückel molecular orbital (EHMO) calculations and experimentally by UV–visible, emission, and polarized emission spectroscopy. The complex is found to be fluorescent at 77 K ($\tau_F = 2.23 \pm 0.03$ ns, $\Phi_F = (2.7 \pm 0.3) \times 10^{-3}$), where no emission attributable to phosphorescence has been observed. This is the first example reported in the $d^{10}-d^{10}$ dimer family. According to the EHMO model, the lowest energy excitation arises from an intraligand π system involving some of the metal atomic orbitals to a π^* system almost entirely localized in the nitrogen frames (i.e. $\pi \rightarrow \pi^*$, $a_u \rightarrow b_{2u}$) with some weak metal-to-ligand charge transfer character, i.e. MLCT; ($^1\text{Ag} \rightarrow ^1\text{B}_{2g}$). The Cu_2 dimer excitation and fluorescence spectra exhibit some vibrational features which were analyzed by time-dependent theoretical calculations. The excited state distortion (ΔQ) calculated for the two dominant Franck–Condon active modes (1400 and 480 cm^{-1}) is 0.050 and 0.067 Å, respectively. Vibrational spectra exhibit peaks at 1368 (Raman and IR) and at 516 (Raman) and 480 cm^{-1} (IR), near the ones calculated, assigned to $\nu(\text{NN})$ and $\nu(\text{CuN})$, respectively. The sign of the ΔQ values is discussed on the basis of the EHMO results and is consistent with a $\pi \rightarrow \pi^*$ intraligand/MLCT model.

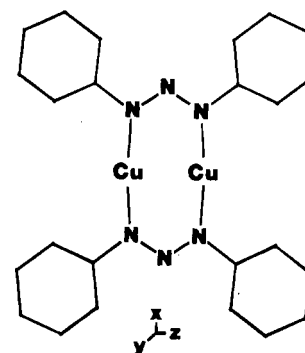
Introduction

The spectroscopic and photophysical properties of polynuclear complexes using d^{10} metal atoms were recently reviewed for $M = \text{Pd}^0, \text{Pt}^0$ ^{1a} and for $M = \text{Cu}^I, \text{Ag}^I, \text{Au}^I$.^{1b} Many of these compounds are found to be strongly luminescent in the solid state, in solution at 77 K, and occasionally in solution at room temperature.¹ Some of these complexes are also known to be powerful photoreducing agents.² The nature of the emitting excited states can vary from metal-to-ligand charge transfer (MLCT) to ligand-to-ligand charge transfer (XLCT when halides and π ligands are used), to metal–metal such as $^3(d\sigma^*p\sigma)^*$, often encountered in binuclear species, and to metal halide-to-ligand charge transfer (M/XLCT) as recently demonstrated.^{1b} The common denominator is that all these emissions come from triplet states and that no fine structure in the emission band has been observed at 77 K, except for a recent report on a tetranuclear copper complex where some weak features were observed at very low temperature.³ In this work we wish to report the spectroscopic properties of the first example of a fluorescent $d^{10}-d^{10}$ species, $\text{Cu}_2(\text{C}_6\text{H}_5\text{NNNC}_6\text{H}_5)_2$ (Chart 1). The compound and the silver analogue were known for some time ($M = \text{Cu}$,⁴ Ag ⁵), but related compounds only recently attracted attention from a theoretical point of view⁶ in order to address the possibility of weak metal–metal interactions. This paper discusses the nature of the luminescent excited states via extended Hückel molecular orbital calculations and the excited state distortions (for $M = \text{Cu}$) and briefly reports the anomalies in the comparison between the absorption and excitation spectra.

[Ⓞ] Abstract published in *Advance ACS Abstracts*, April 1, 1995.

- (1) (a) Harvey, P. D. *J. Cluster Sci.* **1993**, *4*, 377. (b) Piché, D.; Harvey, P. D. *Can. J. Chem.* **1994**, *72*, 705.
- (2) (a) Che, C.-M.; Yip, H. K.; Yam, V. W.-W.; Cheung, P.-Y.; Lai, T.-F.; Shieh, S.-J.; Peng, S. M. *J. Chem. Soc., Dalton Trans.* **1992**, 427. (b) Che, C.-M.; Kwong, H. L.; Poon, C.-K.; Yam, V. W.-W. *J. Chem. Soc., Dalton Trans.* **1990**, 3215.
- (3) Lai, D. C.; Zinc, J. I. *Inorg. Chem.* **1993**, *32*, 2594.
- (4) Brown, I. D.; Dunitz, J. D. *Acta Crystallogr.* **1961**, *14*, 480.
- (5) Beck, J.; Strähle, J. Z. *Naturforsch.* **1986**, *4*, 41B.
- (6) Cotton, F. A.; Feng, S.; Matusz, M.; Poli, R. *J. Am. Chem. Soc.* **1988**, *110*, 7077.

Chart 1. Molecular Structure of $\text{Cu}(\text{C}_6\text{H}_5\text{NNNC}_6\text{H}_5)_2$ (D_{2h} Symmetry) Showing the Molecular Axis Employed



Experimental Section

Materials. The complexes were prepared according to literature procedures.⁴ The phenyl triazide compound ($\text{C}_6\text{H}_5\text{NNN}(\text{H})\text{C}_6\text{H}_5$) was purchased from Aldrich Chemical Co. and was used as received. 2-Methyltetrahydrofuran (2-MeTHF; Aldrich), ethanol (Fisher), butyronitrile (Aldrich), and methylcyclohexane (Fisher) were purified by procedures outlined in refs 7 and 8.

Spectroscopic Measurements. The absorption spectra were measured on a Hewlett Packard 8452 A diode array spectrometer. The luminescence (emission and excitation) spectra were obtained on a double-monochromator Spex Fluorolog II spectrometer or a PTI LS 100 spectrometer. The fluorescence lifetimes were measured with a PTI (Photon Technology Inc.) single-photon counting fluorometer using a $\text{N}_2(\text{g})$ flash-lamp source kept at 15 pKa of pressure. The electrode gap was 1.6 mm operating at 4.0 kV with a repetition rate of 40 kHz. The bandwidth at half-maximum for the lamp decay was 2.5 ns.

Experimental Procedures. The emission quantum yields (Φ) were measured using 9,10-diphenylanthracene as standard.⁹ The polarization

- (7) Perrin, D. D.; Armbrago, W. L. F.; Perrin, D. R. *Purifications of Laboratory Chemicals*; Pergamon: Oxford, U.K., 1966.
- (8) Gordon, A. J.; Ford, R. A. *The Chemist's Companion: Handbook of Practical Data, Techniques and References*; Wiley: New York, 1972.
- (9) Lim, E. C.; Laposz, J. D.; Yu, J. M. *J. Mol. Spectrosc.* **1966**, *19*, 412 and references therein.

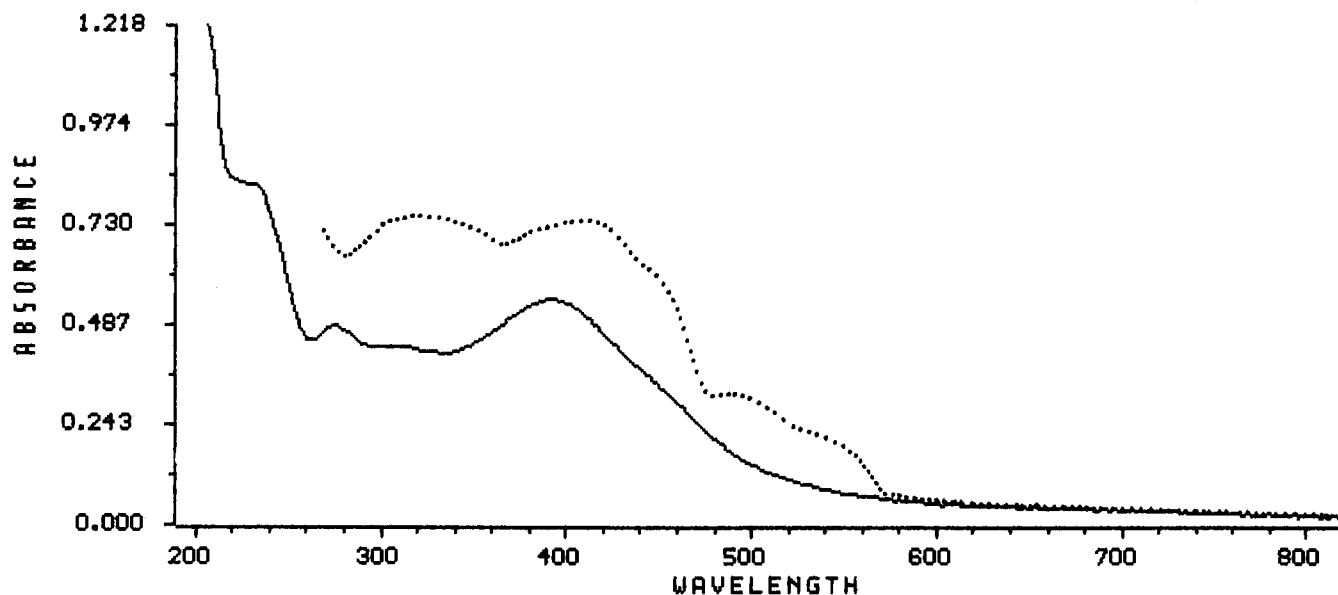


Figure 1. UV-visible spectra of $\text{Cu}_2(\text{C}_6\text{H}_5\text{NNNC}_6\text{H}_5)_2$ in 2-MeTHF at 298 K (—) and at 77 K (···). The 77 K spectrum has not been corrected for glass contraction.

ratios (N) were measured according to literature procedures.^{10,11} The latter experiments were reproduced five times, and in all cases the results were the same.

Computational Details. All MO calculations were of the extended Hückel type (EHMO) using a modified version of the Wolfsberg–Helmholz formula.¹² The atomic parameters used for C, O, H, and N were taken from ref 13. The atomic parameters for Cu are those reported in ref 14. All distances used were the averaged values reported for the X-ray crystallographic structures.^{4,5} A detailed description of the graphic programs used in this work can be found in ref 15. The absorption and excitation spectra were calculated using Heller's dependent theory,¹⁶ giving results equivalent to those of a traditional Franck–Condon analysis.

Results and Discussion

1. Absorption Spectra. The UV-visible spectra (Figure 1) exhibit a maximum at 392 nm where $\epsilon = 7720 \pm 30 \text{ M}^{-1} \text{ cm}^{-1}$ (at 298 K). By comparison with the spectrum of the free ligand (in its protonated form, i.e. $(\text{C}_6\text{H}_5)_2\text{NNN}(\text{H})(\text{C}_6\text{H}_5)$; $\lambda_{\text{max}} = 354 \text{ nm}$, $\epsilon = 20\,110 \pm 40 \text{ M}^{-1} \text{ cm}^{-1}$; ethanol at 298 K), an intraligand $\pi \rightarrow \pi^*$ assignment can be made readily.¹⁷ Some shoulders are also observed on the low-energy side of this band (440 nm, $\epsilon \sim 5000 \text{ M}^{-1} \text{ cm}^{-1}$; 540 nm, $\epsilon \sim 780 \text{ M}^{-1} \text{ cm}^{-1}$), indicating that these bands exhibit some forbidden character. However, these measurements do not allow us to localize the $n \rightarrow \pi^*$ band for which $\epsilon \leq 100 \text{ M}^{-1} \text{ cm}^{-1}$.¹⁸ The latter two observations will be addressed theoretically (EHMO) below.

2. Fluorescence Spectra. Some moderate vibrational structures are observed in the emission spectra ($\Phi = 0.0027 \pm$

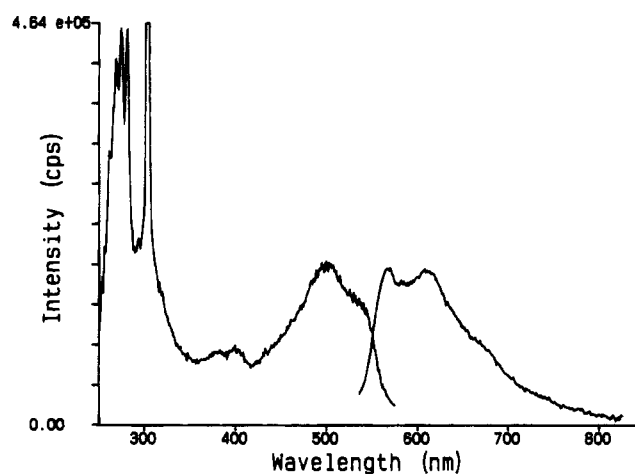


Figure 2. Excitation (left) and emission (right) spectra of $\text{Cu}_2(\text{C}_6\text{H}_5\text{NNNC}_6\text{H}_5)_2$ in 2-MeTHF at 77 K. The sharp peak located at $\sim 300 \text{ nm}$ in the excitation spectrum is an artifact due to the gratings ($\lambda_{\text{emi}} \sim 600 \text{ nm}$ in this measurement; i.e. first harmonic).

0.0003) of the dimer at 77 K (Figure 2). On the basis of the small Stokes shifts ($\leq 1000 \text{ cm}^{-1}$) and emission lifetimes ($2.23 \pm 0.06 \text{ ns}$; $\chi^2 = 1.04$), the observed luminescence is fluorescence, again a property never reported for this family of compounds¹⁹ and considered rare for inorganic and organometallic complexes.²⁰ The radiative ($k_{\text{F}} = \Phi_{\text{F}}/\tau_{\text{F}}$) and nonradiative rate constants ($k_{\text{nr}} = (1 - \Phi_{\text{F}})/\tau_{\text{F}}$) are $1.2 \times 10^6 \text{ s}^{-1}$ and $4.5 \times 10^8 \text{ s}^{-1}$, respectively. The uncertainties are $\sim 10\%$. The k_{F} value is typical of fluorescence behavior,²¹ but k_{nr} suggests that the

- (10) (a) Zelent, B.; Harvey, P. D.; Durocher, G. *Can J. Spectrosc.* **1984**, 29, 23. (b) *Can J. Spectrosc.* **1983**, 28, 188.
- (11) Harvey, P. D.; Zelent, B.; Durocher, G. *Spectrosc., Int. J.* **1983**, 2, 128.
- (12) Ammeter, J. H.; Burgi, H. B.; Thibeault, J. C.; Hoffmann, R. *J. Am. Chem. Soc.* **1978**, 100, 3686.
- (13) (a) Hoffmann, R.; Lipscomb, W. N. *J. Chem. Phys.* **1962**, 36, 2179. (b) *J. Chem. Phys.* **1962**, 37, 2872. Hoffmann, R. *J. Chem. Phys.* **1963**, 39, 1397.
- (14) Hay, P. J.; Thibeault, J. C.; Hoffmann, R., *J. Am. Chem. Soc.* **1975**, 97, 4884.
- (15) Mealli, C.; Proserpio, D. M. *J. Chem. Educ.* **1990**, 67, 399.
- (16) Heller, E. J., *Acc. Chem. Res.* **1981**, 14, 368.
- (17) The decrease of the ϵ values upon going from the free ligand to the dimer could be due to the increase in molecular weight. The $\pi \rightarrow \pi^*$ assignment is also consistent with recent works on dibenzylideneacetone bridging ligands, ligands that are not too different in nature from the $\text{C}_6\text{H}_5\text{NNNC}_6\text{H}_5$ ligand used in this work. See references in footnote 18.

- (18) (a) For the structurally related dibenzylideneacetone bridging ligand $(\text{C}_6\text{H}_5\text{CH}=\text{CH}(\text{CO})\text{CH}=\text{CHC}_6\text{H}_5)$, the $n \rightarrow \pi^*$ band has never been experimentally observed. EHMO calculations have predicted that this state lies near the lowest energy excited state.^{18b-e} (b) Harvey, P. D.; Daoust, B. *Can. J. Chem.* **1992**, 70, 1777. Harvey, P. D.; Aubry, C.; Gan, L.; Drouin, M. *J. Photochem. Photobiol.* **1991**, 57, 465. (c) Harvey, P. D.; Gan, L.; Aubry, C. *Can J. Chem.* **1990**, 68, 2278. (d) Harvey, P. D.; Sharman, G. *Can. J. Chem.* **1990**, 68, 223.
- (19) Preliminary results on the silver analogue $(\text{Ag}_2((\text{C}_6\text{H}_5\text{NNNC}_6\text{H}_5)_2))$ have shown that the luminescence in this case is also fluorescence; λ_{max} (absorption) = 374 nm, $\epsilon = 12\,600 \pm 200 \text{ M}^{-1} \text{ cm}^{-1}$ (with a long tail reaching the 600 nm region), $\lambda_{\text{emi}} = 610 \text{ nm}$ (2-MeTHF, 77 K), and $\tau_e = 2.73 \pm 0.08 \text{ ns}$ ($\chi^2 = 1.08$, 2-MeTHF, 77 K). The emission and absorption spectra are, however, much less structured, where only a weak shoulder on the low-energy side is noticed. No phosphorescence has been observed in this case as well. The metal dependence of the λ values is in agreement with the EHMO results.

intersystem crossing rate constants (k_{isc}) cannot exceed $4.5 \times 10^8 \text{ s}^{-1}$. Such a value is considered to be at the lower limit for k_{isc} and is typical for intersystem crossing between two $\pi\pi^*$ states. The absence of observed emission arising from the triplet state suggests that the spin–orbit coupling between the heavier metal atom and the triplet electronic states is somewhat weak and that the triplet state is not efficiently populated. The fact that τ_F is somewhat long for an inorganic compound^{21a} can be, in part, a consequence of the weak spin–orbit coupling but could also be associated with the low absorptivity of the lowest energy band (due to its orbitally forbidden character).^{21c} The most astonishing result is the lack of complete correspondence between the absorption and excitation spectra where only the low-energy band shows good correspondence. Physically, this result indicates that the photon energy is not completely channeled down to the fluorescent state. This behavior is unusual but not new in the d¹⁰–d¹⁰ series. The related and organometallic M₂(dba)₃ complexes (M = Pd, Pt; dba = dibenzylideneacetone) and substituted derivatives behave similarly.²² This behavior was recently investigated by picosecond and nanosecond flash photolysis spectroscopy,^{22a} and the results were tentatively interpreted by the presence of “energy-wasting” reversible photoinduced *cis*–*trans* isomerization processes occurring with the bridged dba ligand in the upper excited states. This photoisomerization behavior is also known for the free dba ligand and derivatives.^{18c} In this work, there is not yet evidence of photoinduced isomerization. To our knowledge the free ligand has not been investigated in this respect.

The fluorescence band shifts to the red with medium polarity (positions of the apparent 0–0 band are 560, 561, 567, and 575 nm, for methylcyclohexane, toluene, 2-methyltetrahydrofuran, and butyronitrile, respectively, solvents in which the dimer is soluble), indicating that the fluorescence must arise from a $\pi \rightarrow \pi^*$ transition and unambiguously rules out the possible (N=N) $n \rightarrow \pi^*$ assignment. The polarization ratios of the Cu₂ fluorescence spectrum have been measured in order to address the possibility of different excited states that would be responsible for the absorption and emission, respectively, ($n\pi^*$ vs $\pi\pi^*$), and to detect the presence of different Franck–Condon active modes with different symmetries (if any), particularly when the absorptivities are low in the 500 nm absorption range. The polarization ratio, N , is given by $(I_{BB}/I_{BE})_V(I_{EE}/I_{EB})_H$, where $(I_{BB}/I_{BE})_V$ is the ratio of the intensities of vertically to horizontally polarized emission when excited with vertically polarized light and $(I_{EE}/I_{EB})_H$ is the ratio of the intensities of ||- and ⊥-polarized emission with horizontally polarized excitation. N is then related to the relative orientation of the transition moments in absorption and emission. The theoretical value of $N = 3$ indicates that absorption polarized on a single molecular

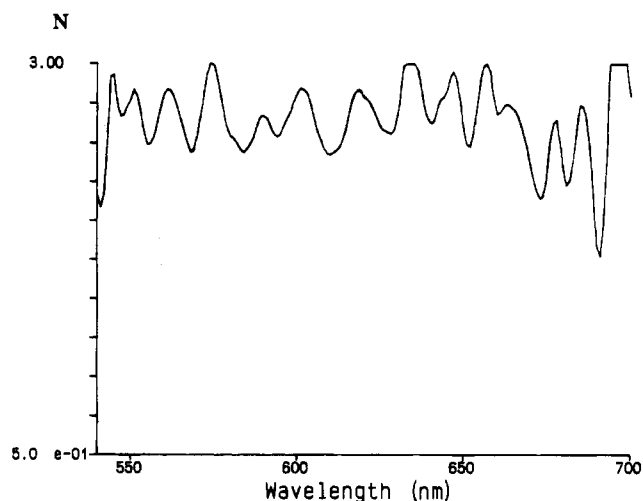


Figure 3. Polarization ratio (N) measured as a function of λ along the fluorescence spectrum of Cu₂(C₆H₅NNNC₆H₅)₂ (2-MeTHF at 77 K).

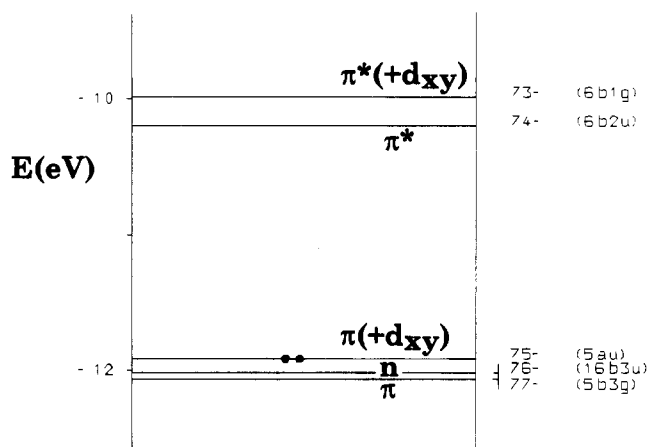


Figure 4. EHMO energy levels for the frontier orbitals in the Cu₂(C₆H₅NNNC₆H₅)₂ complex. The LUMO and HOMO are MO's 74 and 75, respectively.

axis is followed by emission along the same axis. $N = 0.5$ indicates that single-axis absorption is followed by emission along a perpendicular axis. In practice, the theoretical values were never obtained due in part to the natural depolarization of the glass. The experiment shows an average value of 2.8 all along the fluorescence spectrum when the excitation is at 500 nm (Figure 3) and all along the excitation spectrum between 450 and 550 nm (at $\lambda_{emi} = 600$ nm), clearly indicating that the emission (600 nm) is polarized parallelly to the absorption (500 nm). The 500 nm absorption band is assigned to a $\pi \rightarrow \pi^*$ transition. The constant N value (along the spectrum) indicates that the symmetry of the Franck–Condon active modes is the same all along the progression. The graph of N vs λ shows some fluctuation (i.e. noise) that is associated with the smaller emission quantum yield ($\Phi_F = 0.0027$). The 400 nm excitation experiment was not attempted since the correspondence between absorption and excitation is not adequate in this region; the N values would be physically meaningless.

3. EHMO Analysis. Two closely related compounds (M₂(C₆H₅NCHNC₆H₅)₂) were recently investigated by SCF–X α –SW theoretical calculations.⁶ The two major differences with this work are that (1) the previous calculations did not take into account the presence of the phenyl groups and (2) the N₃ groups exhibit free lone pairs potentially giving rise to $n \rightarrow \pi^*$ transitions close in energy to the lowest energy absorption. A MO diagram is generated using the EHMO model (and the structural data for Cu₂(C₆H₅NNNC₆H₅)₂; D_{2h} point group;⁴ Figure 4). The LUMO (MO 74; b_{2u}) is essentially the same as

- (20) (a) Examples of fluorescent inorganics exist and include porphyrin compounds^{20b} and some iridium complexes.^{20b} (b) See, for example: Sessler, J. L.; Johnson, M. R.; Lin, T.-Y.; Creager, S. E. *J. Am. Chem. Soc.* **1988**, *110*, 3659. (c) Balch, A. L.; Nagle, J. K.; Oram, D. E.; Reedy, P. E. *J. Am. Chem. Soc.* **1988**, *110*, 454.
- (21) (a) See for instance the data reported for the Pt₂(POP)₄⁴⁻ complex, for which both emissions arising from the singlet and triplet states are observed ($\tau_F = 8$ ps; $k_F = 2 \times 10^7 \text{ s}^{-1}$): Stigman, A. R.; Rice, S. F.; Gray H. B.; Miskowski, V. M. *Inorg. Chem.* **1987**, *26*, 1112. (b) Turro, N. J. *Modern Molecular Photochemistry*; Benjamin/Cummings: Menlo Park, CA, 1978. (c) The theoretical fluorescence rate constant, $k_F^{(T)}$, can be roughly estimated using the oscillator strength concept:^{21b} $f = 4.3 \times 10^9 \int \epsilon \, d\nu$; $k_F^{(T)} = 3 \times 10^{-9} \bar{\nu}_0^2 f \epsilon \, d\nu$. To estimate $f \epsilon \, d\nu$, the triangle method is used where $\epsilon = 780 \text{ M}^{-1} \text{ cm}^{-1}$, and the width at half maximum is 4870 cm^{-1} extracted from the excitation spectrum. Using $\bar{\nu}_0 = 20\,000 \text{ cm}^{-1}$, $k_F^{(T)} = 4.6 \times 10^6 \text{ s}^{-1}$. This crude comparison is not perfect, but the data are in the right order of magnitude.
- (22) (a) Hubig, S. M.; Drouin, M.; Michel, A.; Harvey, P. D. *Inorg. Chem.* **1992**, *31*, 5375. (b) Harvey, P. D.; Gray, H. B. *Polyhedron* **1990**, *9*, 1949. (c) Harvey, P. D.; Adar, F.; Gray, H. B. *J. Am. Chem. Soc.* **1989**, *111*, 1312.

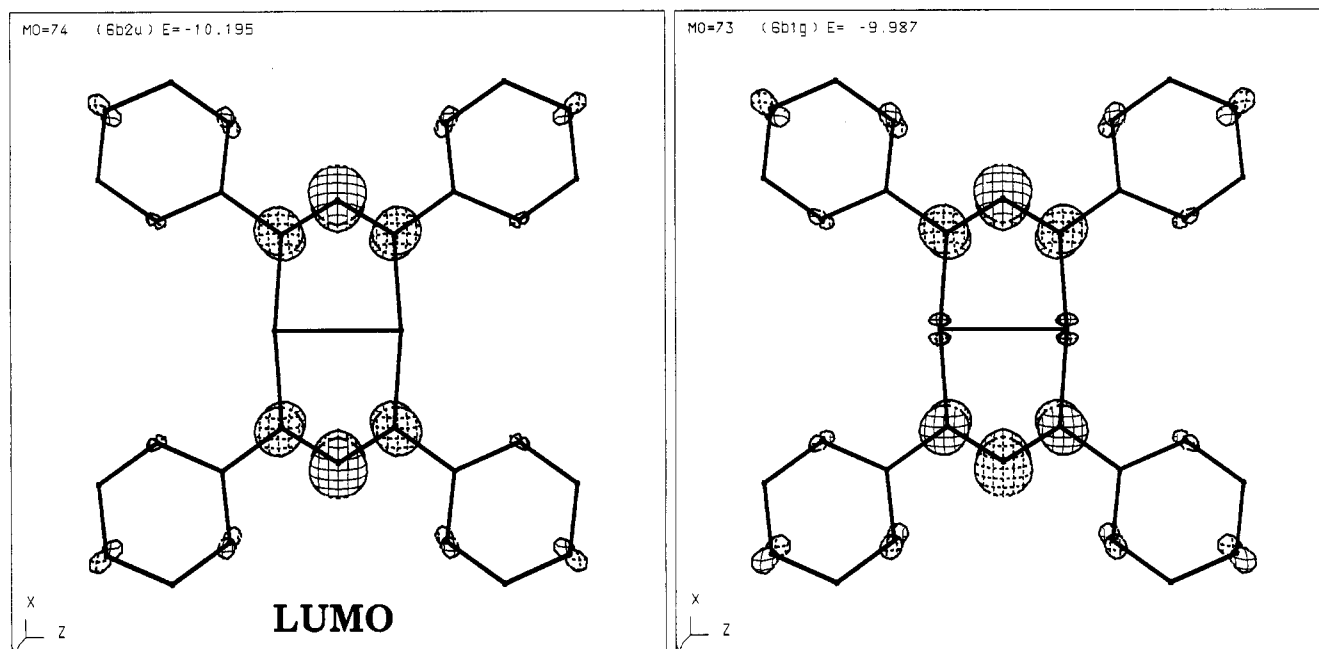


Figure 5. MO pictures for the LUMO (74) and LUMO + 1 (73).

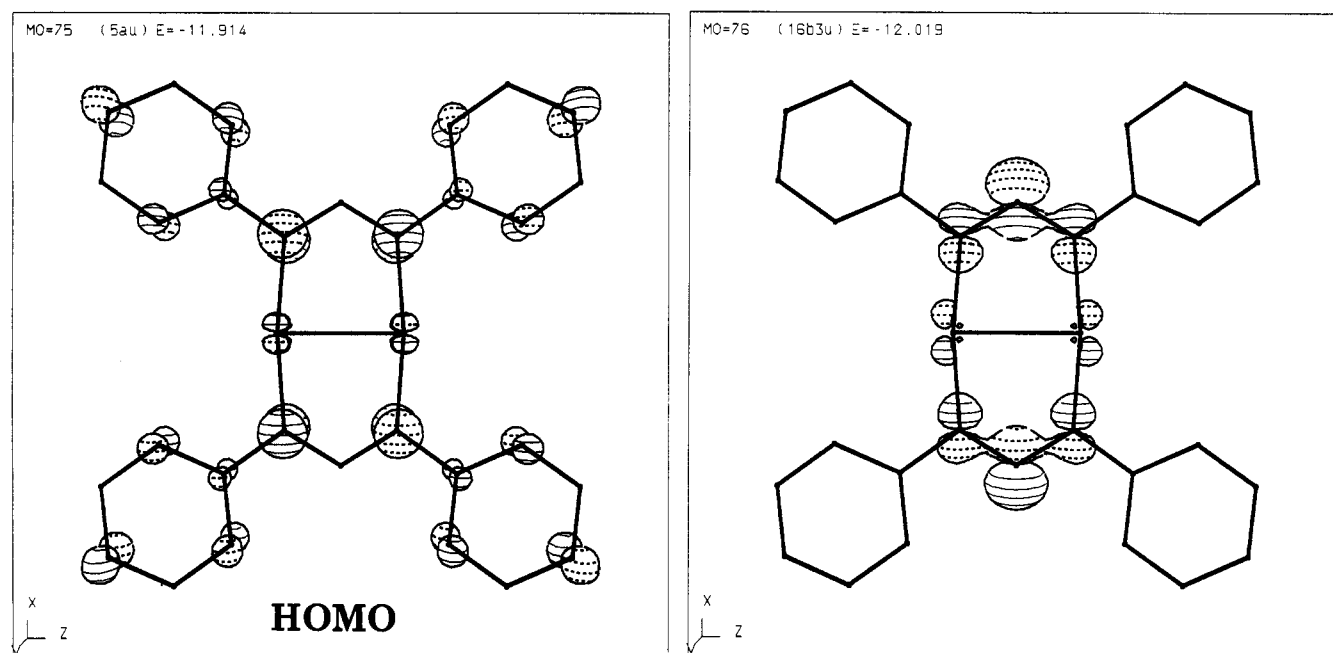


Figure 6. MO pictures for the HOMO (75) and HOMO - 1 (76).

Table 1. Atomic Contributions (%) for the $\text{Cu}_2(\text{C}_6\text{H}_5\text{NNNC}_6\text{H}_5)_2$ Complex

MO no.	atomic contributions				comments	
73 (6b _{1g})	N(p _y)	C(p _y)	Cu	others	π^* centered on N atoms	
	76	16	4	4		
74 (6b _{2u})	N(p _y)	C(p _y)	Cu	others	π^* centered on N atoms, LUMO	
	40	52	6	2		
75 (5a _u)	N(p _y)	C(p _y)	Cu(d _{xy})	others	π system (with little metal contribution), HOMO	
	78	0	12	10		
76 (16b _{3u})	N(p _x)	C(p _x)	Cu(p _x)	others	n(N)	
	78	0	12	10		
77 (5b _{3g})	N(p _y)	C(p _y)	Cu	others	π system (intraligand)	
	32	60	2	6		

reported for the $\text{M}_2(\text{C}_6\text{H}_5\text{NCHNC}_6\text{H}_5)_2$ complexes ($\text{M} = \text{Cu}$, Ag) and is a π^* system, largely located in the N_3 center with very little M atomic contributions (see Table 1 and Figure 5 for details). The LUMO + 1 (MO 73) lies about 0.2 eV above the LUMO, a MO that exhibits similar atomic contributions to the LUMO with the exception of the orbital symmetry (b_{1g} ; Figure 5). The HOMO (MO 75; $5a_u$) is located about 1.72 eV

(i.e. $\sim 18\,900\text{ cm}^{-1}$) under the LUMO and is composed of a π -bonding system distributed in the phenyl and N_3 groups (Figure 6), including a small but nonnegligible amount of d_{xy} . Cu atomic contributions (6%; Table 1). This result is also in agreement with the SCF-X α -SW calculations for the $\text{M}_2(\text{C}_6\text{H}_5\text{NCHNC}_6\text{H}_5)_2$ complexes ($\text{M} = \text{Cu}$, Ag);⁶ i.e. the HOMO is a_u , but the metal atomic contributions to the MO are much higher

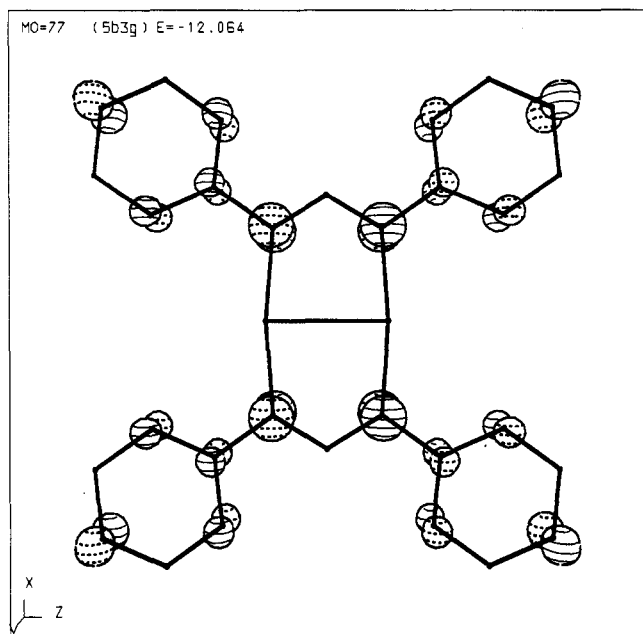


Figure 7. MO picture for MO 77 (i.e. the $5b_{3g}$ MO).

for $M = \text{Cu}$ (38%) and are reasonably comparable for $M = \text{Ag}$ (11%). The metal angular contribution is in all cases (this work and previous work⁶) the same (100% d_{xy}). This difference cannot be easily explained and appears to be related to the methods employed for the computations. Below the HOMO lie two MO's (MO's 76 and 77) at 0.11 eV ($\sim 850 \text{ cm}^{-1}$) and 0.15 eV ($\sim 1210 \text{ cm}^{-1}$), respectively. The former is almost exclusively composed of N p_x atomic orbitals (78%) which are essentially the N lone pairs (Figure 6). Some Cu p_x atomic contributions (12%) are also noted, and these promote bonding interactions between the metal and the ligand. The symmetry of this orbital is b_{3u} , and the lowest energy $n \rightarrow \pi^*$ transition ($b_{3u} \rightarrow b_{2u}$) is forbidden as group theory would predict. On the other hand, the other $n \rightarrow \pi^*$ transition is the $b_{3u} \rightarrow b_{1g}$ (MO 73) transition which is allowed (and polarized along the y molecular axis). Due to the orthogonality of these MO's, the band intensity associated with this transition is not expected to be great. The last MO orbital noted (MO 77; symmetry = b_{3g}) is similar in composition to the HOMO (Table 1) where the electronic density is distributed on the phenyl and N_3 groups (Figure 7). Some very weak metal contribution is computed ($\sim 2\%$). The $5b_{3g} \rightarrow 6b_{2u}$ transition is allowed and should be more energetic than the $5a_u \rightarrow 6b_{2u}$ by about 0.15 eV.

The 0-0 band observed at $\sim 560 \text{ nm}$ (i.e. $\sim 17860 \text{ cm}^{-1}$, 2.21 eV) compares reasonably with the EHMO HOMO-LUMO gap (1.72 eV) with a difference of about 22%, which is not unusual with the computational method employed.

The MO ordering (Figure 4) appears to be the correct one. The LUMO is b_{2u} , as the SCF-X α -SW calculations on related compounds predict the same result.⁶ In this previous work, no evidence of a close-lying MO (near the LUMO) was reported.⁶ On the basis of the blue shift of the fluorescence band with the medium polarity, the associated electronic transition is not $n \rightarrow \pi^*$ but is rather consistent with a $\pi \rightarrow \pi^*$ transition. Due to low absorption around 550 nm ($\epsilon \sim 780 \text{ M}^{-1} \text{ cm}^{-1}$ at 540 nm; Figure 1), the electronic transition is definitely forbidden by symmetry ($a_u \rightarrow b_{2u}$ is forbidden; $b_{3g} \rightarrow b_{2u}$ is not). Finally MO's 76 and 77 are very close in energy (0.045 eV; 360 cm^{-1}) and cannot be easily addressed experimentally. These can be inverted but are of very little consequence for this work.

4. Franck-Condon Analysis. The lowest energy electronic transition ($a_u \rightarrow b_{2u}$) exhibits a migration of some electronic density from both the phenyl groups and the copper metals to

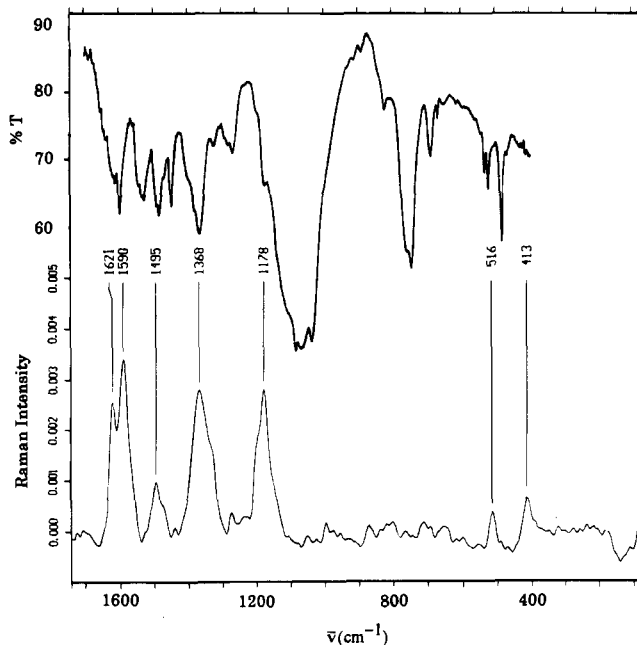


Figure 8. Top: FT-IR spectrum of solid $\text{Cu}_2(\text{C}_6\text{H}_5\text{NNNC}_6\text{H}_5)_2$ in the $400\text{--}1740 \text{ cm}^{-1}$ range (resolution 4 cm^{-1} ; 200 scans). Bottom: FT-Raman spectrum of solid $\text{Cu}_2(\text{C}_6\text{H}_5\text{NNNC}_6\text{H}_5)_2$ at 298 K. Experimental conditions: resolution, 4 cm^{-1} ; number of scans, 1500; laser excitation, 1064 nm; laser power at the sample, 51 mW (defocused); baseline-corrected spectrum. Proposed assignments: 1621, 1590, and 1495 cm^{-1} , $\nu(\text{CC})$; 1368 cm^{-1} and a shoulder at 1340 cm^{-1} , $\nu(\text{NN})$ ($a_g + b_{3g}$); 1178 cm^{-1} , $\nu(\text{NC})$ or $\nu(\text{CC})$; 516 and 413 cm^{-1} , $\nu(\text{CuN})$ ($a_g + b_{3g}$). The region above 1740 cm^{-1} was not investigated and exhibited only the C-H stretching bands.

the N_3 centers. Therefore the $\pi \rightarrow \pi^*$ nature of the transition is mixed with a minor contribution of metal-to-ligand charge transfer (MLCT). Such a conclusion is supported by the larger red shift of the λ_{max} (of emission) with the medium polarity, with respect to typical $\pi \rightarrow \pi^*$ electronic bands.^{21b} The lowest energy bands for the d^{10} - d^{10} $\text{M}_2(\text{dba})_3$ complexes ($M = \text{Pd}$, Pt) have also been assigned to MLCT.²² In the latter cases, the MLCT nature of the excited states appears to be more pronounced.

The vibrational structure of the excitation (rather than the absorption)²³ and the emission bands were analyzed using Heller's time-dependent theory.¹⁶ An attempt to define a model using the lowest number of parameters to correctly calculate the experimental spectra, consisting of two-dimensional harmonic oscillator potential energy surfaces for both the ground and excited electronic states, was made. No satisfactory result was obtained using a single Franck-Condon active mode. In the two-mode model, the vibrational frequencies were held fixed at 1400 and 480 cm^{-1} , close to the vibrational frequencies observed in the vibrational spectra (see Figure 8). A variation of these frequencies by 10% does not lessen the agreement between calculated and experimental spectra, showing only large vibronic bands and no discernible peaks for the individual modes. The Huang-Rhys parameters, S ,²⁴ for both vibrational modes were treated as adjustable parameters in the fitting process, using the entire emission spectra and the region from 18 000 to 21 500 cm^{-1} of the excitation spectrum. The agreement between calculated and experimental spectra (Figure 9) is excellent in view of the simple model with only two

(23) There is significant overlap between the different and closely located absorption bands (Figure 1). The excitation spectra do not display such behavior where the lowest energy band is reasonably isolated. The comparison between a calculated and an observed spectrum is more appropriate in this case.

(24) Huang, K.; Rhys, A. *Proc. R. Soc. London* **1958**, A204, 406.

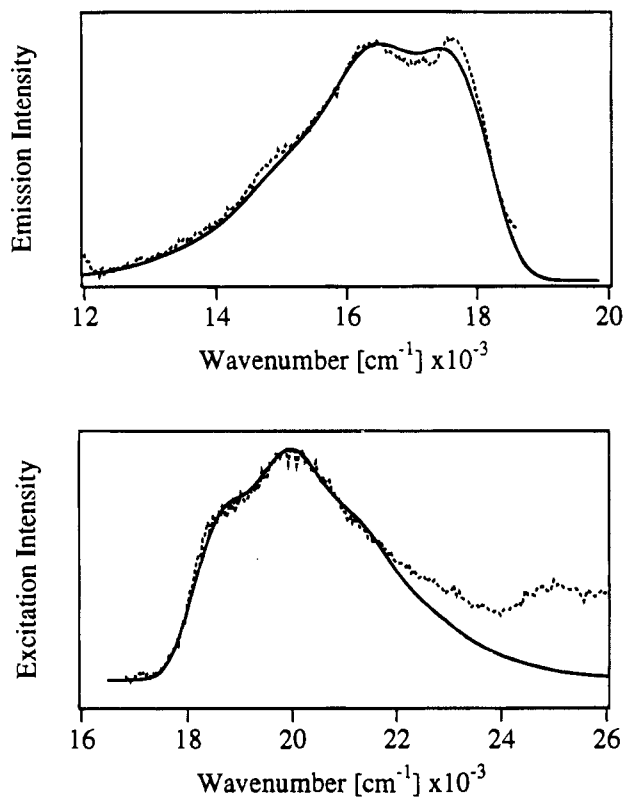
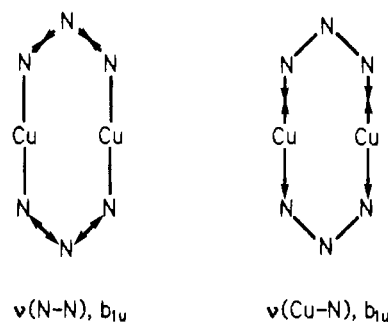


Figure 9. Comparison between the calculated (—) and experimental spectra (···) for the fluorescence (upper) and excitation spectra (lower) of Figure 2 using time-dependent Heller's theory.

adjustable parameters. Values of 0.84 and 0.95 were obtained for S along the 1400 and 480 cm^{-1} modes, respectively. The estimated uncertainties of these values are on the order of 10%. These modes are easily assigned to $\nu(\text{NN})$ (1368 Raman and IR) and $\nu(\text{CuN})$ (516 Raman, 480 cm^{-1} IR).²⁵ We conclude that the emitting state of the Cu_2 compound is distorted along at least one high-frequency ($\nu(\text{NN})$) and one low-frequency ($\nu(\text{CuN})$) normal coordinate. Group theory predicts that the four vibrational modes for each of the N–N and Cu–N bonds transform as $\Gamma_{\text{N-N}} = \Gamma_{\text{Cu-N}} = a_g + b_{3g} + b_{1u} + b_{2u}$. Since the electronic transition $a_u \rightarrow b_{2u}$ (i.e. ${}^1A_g \rightarrow {}^1B_{2g}$) is forbidden ($\epsilon \sim 780 \text{ M}^{-1} \text{ cm}^{-1}$ at 295 K), vibronic coupling must be important to explain the vibrational progression intensity. Interestingly, first-order perturbation theory ($\int \psi_e \psi_v \mu_e |\psi_e' \psi_v' d\tau$;^{21b} $\psi_e = {}^1A_g$, $\psi_v = a_g$ for absorption, $\mu_e = T_x(b_{3u})$, $T_y(b_{2u})$, $T_z(b_{1u})$, $\psi_e' = {}^1B_{2g}$ and $\psi_v' =$ perturbing vibrational mode in the excited state) predicts that the wavefunction symmetry for the perturbing modes should be a_u (y -polarized), b_{1u} (x -polarized), and b_{3u} (z -polarized). For the $\nu(\text{N-N})$ and $\nu(\text{Cu-N})$ modes, clearly the b_{1u} modes (IR active) can act as the Franck-Condon active modes in the lowest energy ${}^1B_{2g}$ state. The schematic representations of the b_{1u} atomic displacements for $\nu(\text{N-N})$ and $\nu(\text{Cu-N})$ are shown in Chart 2. Experimentally, the constant N values along the emission and excitation spectra (Figure 3) strongly support this prediction. The position of the calculated 0–0 band using Heller's theory is 18 200 cm^{-1} (550 nm), a position where both low-energy fluorescence and excitation bands meet (Figure 2). The intensity of excitation and emission at this position is about half the intensity of the first shoulder ($\sim 540 \text{ nm}$) and band ($\sim 560 \text{ nm}$), respectively, what was the

Chart 2



“apparent 0–0”. If the true 0–0 band could have been resolved, its intensity would not have been great. This observation explains why no clear change in polarization ratios is observed upon going from 550 to 600 nm. The closest peaks observed in the IR spectra are 1368 and 480 cm^{-1} and compare reasonably well with the calculations. The excited state distortions (ΔQ) are calculated^{16,24} and are 0.050 and 0.067 \AA for the two modes, respectively. These values compare favorably with the data reported for the $\text{Ru}(\text{bpy})_3^{2+}$ cation (bpy = bipyridine) for which a lowest energy metal-to-ligand charge transfer excited state is assigned.²⁶ In this case, ΔQ average $\sim +0.07 \text{ \AA}$, along the C–C bonds in the bpy ligands.²⁶ Recently Lai and Zinc³ calculated ΔQ for a complex $\text{Cu}_4\text{L}_4(\text{dmpp})_4$ in its triplet state (dmpp = 1-phenyl-3,4-dimethylphosphole) which was assigned to a MLCT state as well. In this case ΔQ is 0.06 \AA also along the C=C bond.

The HOMO is antibonding in Cu–N interactions and nonbonding in $\text{N}\cdots\text{N}$ interactions (Figure 6). The LUMO is antibonding in the N_3 frame and has very little Cu atomic contributions (Figure 5). In the ${}^1(a_u)({}^1b_{2u})$ excited state, the Cu–N bonds are expected to shrink, which is perfectly consistent with a MLCT character, while the N–N distances are predicted to increase, with respect to the ground state. The signs of the ΔQ values are negative (-0.050 \AA) and positive ($+0.067 \text{ \AA}$), respectively. High-resolution UV–visible and emission spectroscopy would have been useful to confirm these data if such spectra could have been obtained.

There has been no evidence for $\text{Cu}\cdots\text{Cu}$ interactions in this work, despite the fact that the $\text{Cu}\cdots\text{Cu}$ distance ($d(\text{Cu}\cdots\text{Cu})$) is $2.45 \pm 0.02 \text{ \AA}$,⁴ a distance that is well within the sum of both the covalent (1.28 \AA) and the van der Waals radii (1.40 \AA).²⁷ The relatively modest metal atomic contributions to the HOMO and LUMO are consistent with this observation (as far as the excited states are concerned). $\nu(\text{Cu}_2)$ still needs to be localized in the Raman spectra. On the basis of the vibrational data²⁸ reported for $\text{Cu}(\text{O}_2\text{CCH}_3)_4 \cdot 2\text{H}_2\text{O}$ ($d(\text{Cu}\cdots\text{Cu}) = 2.491 \text{ \AA}$) and related compounds,²⁹ $\nu(\text{Cu}\cdots\text{Cu})$ should have been observed between 250 and 170 cm^{-1} . Presumably this Raman band is somewhat weaker than the Cu–N stretching ones shown in Figure 8.

Acknowledgment. This research was supported by the NSERC and FCAR. P.D.H. thanks Professor C. Reber (Université de Montréal) for the time-dependent theoretical calculations and Mr. J. Gagnon and Mr. R. Provencher for technical assistance.

IC9407149

(25) Nakamoto, K. *Infrared and Raman Spectra of Inorganic and Coordination Compounds*, 4th ed.; Wiley: New York, 1986. The IR-active peaks are as follows (in cm^{-1}): $\sim 1600 \text{ m}$, 1550 m , 1492 m , 1460 m , 1369 m , 1260 s , 1096 vs , 807 w , 794 ms , 683 m , 525 w , 515 w , 480 m . These are not assigned except for those discussed in the text.

(26) Dallinger, R. F.; Woodruff, W. H. *J. Am. Chem. Soc.* **1979**, *101*, 1355.
 (27) Cotton, F. A.; Wilkinson, G.; Gaus, P. L. *Basic Inorganic Chemistry*; p 60.
 (28) San Filippo, J., Jr.; Sniadoch, H. *J. Inorg. Chem.* **1973**, *12*, 2326.
 (29) Iijima, K.; Itoh, T.; Shibata, S. *J. Chem. Soc., Dalton Trans.* **1985**, 2555.